EPRI/STANFORD/USGS WORKSHOP
EARTHQUAKE GROUND MOTION AT CLOSE DISTANCES

September 5,6, 1990
Stanford University

Stephen Hartzell

U.S. Geological Survey
Branch of Geologic Risk Assessment
Box 25046, MS 966
Denver, CO 80225

Thomas Heaton

U.S. Geological Survey
Seismology Branch
525 South Wilson Ave.
Pasadena, CA 91106

San Andreas Deterministic Fault Problem
Green's Function Summation for a Finite Source

Ground motion synthetics (displacement, velocity and acceleration) are calculated for the proposed San Andreas earthquake using the technique of summation of Green's functions. The frequency range of our calculations is from 0. to 25. Hz. Most of the parameters of the earthquake are specified in the exercise. However, variation in the models is allowed for in three primary areas: 1) the type of Green's functions to be summed, theoretical or empirical, 2) randomness in the model, and 3) the nature of the source-time-function. We will concentrate the discussion of our modeling effort on these three topics.

Green's Functions

We use a two fold method of ground motion simulation. In the frequency range from 0. to 2. Hz discrete wavenumber/finite element, full-wave-theory Green's functions (Olson *et al.*,1984) are calculated for the specified velocity model and summed over the finite fault. In the frequency range from 2. to 25. Hz we add the ground motion recorded for a similar moment magnitude earthquake observed at a similar fault-station geometry. These two halves of the simulation are joined together by symmetric lowpass and highpass-butterworth filters with corners at 2. Hz. The upper limit of 25. Hz is the Nyquist frequency obtained from the time sampling of 0.02 sec of the observed ground motion record.

One advantage of using the discrete wavenumber/finite element Green's functions is the accurate representation of long-period motions and static offsets near the fault. Some of the Green's functions are shown in Figures 1a and b for two extremes in source depth and a dip-slip mechanism. In total Green's functions were calculated for 16 source depths (1, 2, 3, 4, 5, 6, 7, 8, 9, 10, 11, 12.5, 14, 15.5, 17, and 18.5 km) and 29 ranges (1, 2, 3, 4, 5, 7, 9, 11, 13, 15, 17, 19, 22, 25, 28, 31, 34, 37, 40, 45, 50, 55, 60, 65, 70, 75, 80, 85, and 90 km). Bi-linear interpolation of the Green's functions on the S-wave time is used to calculate the response of a finite fault from the set of Green's funcitons with specific source depths and ranges (Hartzell and Heaton, 1983). The point source spacing on the fault plane is 0.235 km along the length of the fault and 0.190 km down the fault width. Therefore, each synthetic represents the summation of 32704 point sources.

To simulate the high-frequency ground motion one could sum high-frequency synthetic or empirical Green's functions. We have chosen to add a single highpassed ground motion record to represent this frequency band. By using this procedure we avoid the uncertainties involved in specifying the randomness of the high-frequencies. The record we have chosen is the Tabas strong motion record for the 1979 Tabas, Iran, earthquake. The Tabas earthquake has a surface-wave magnitude of 7.4 and a body-wave magnitude of 6.5. The Tabas station has a similar relationship to the fault plane and the hypocenter as the site in the proposed problem. Before adding the Tabas ground motion it is scaled using the distance attenuation relationship of Joyner and Boore (1981).

Fault Randomness

We have included randomness in the rupture times of the point source summation which has the same character suggested by the inversion results of Hartzell (1989) and Hartzell and Iida (1990) for earthquakes in southern California. Figure 2 shows contours of the rupture front at 3 sec intervals. The figure has a 2X vertical exaggeration. Randomness is added in a controlled manner. A random factor of ±1 sec is added to the rupture times on a grid work of points with 31 points along the strike and 10 points down the dip. Bi-linear interpolation is then used to calcaulate the rupture times of intermediate point sources. The net effect is to produce a rupture which propagates at an average velocity of 3.0 km/sec but which has local variations in rupture time of ±1 sec.

Source-Time-Function

We assume a constant source-time-function or slip function on the fault. The over-all duration of the time function is set by the requirement that the maximum source velocity be about 1 meter/sec. For the proposed problem with a uniform slip distribution, the slip on the fault is about 4.5 meters. We have therefore set the duration of the source-time-function at 4 sec. A simple triangular time function was first considered. However, use of this function led to large spectral holes in the amplitude spectrum of the ground motion. The more broadband time function shown in Figure 2 is considered more realistic and is the one used in our synthetics. This time function is similar to an idealized Kostrov (1964) function with a sharp onset and long-period tail.

Synthetic Results

The synthetic waveforms are shown in Figure 3 for uniform fault slip and Figure 4 for the non-uniform slip model. For both of these models displacement, velocity, and acceleration records are shown for first a site 5 km from the frault trace, and second a site 10 km from the fault trace. All the simulated ground motions are plotted at 5 sec/inch and start at the origin time of the earthquake. Peak ground motion values are given below each trace in units of cm, cm/sec, and cm/sec^2. The ground motions are potentially very destructive. They show large accelerations (approaching-1.0g) and large static displacements (near 1.0 meter) occurring over a time interval of 10 seconds. The large displacements could be particularly damaging to base-isolated structures.

References

Hartzell, S. H., and T. H. Heaton (1983). Inversion of strong ground motion and teleseismic waveform data for the fault rupture history of the 1979 Imperial Valley, California, earthquake, *Bull. Seism. Soc. Am.*, 73, 1553-1583.

Hartzell, S. H. (1989). Comparison of seismic waveform inversion results for the rupture history of a finite fault: application to the 1986 North Palm Springs , California, earthquake, *J. Geophys. Res.*, 94, 7515-7534.

Hartzell, S. H., and M. Iida (1990). Source complexity of the 1987 Whittier Narrows, California, earthquake from the inversion of strong motion records, *J. Geophys. Res.*, 95, 12,475-12,485.

Joyner, W. B., and D. M. Boore (1981). Peak horizontal acceleration and velocity from strong-motion records including records from the 1979 Imperial Valley, California, earthquake, *Bull. Seism. Soc. Am.*, 71, 2011-2038.

Kostrov, B. V. (1964). Self-similar problems of propagation of shear cracks, *J. Appl. Math. Mech.*, 28, 1077-1087.

Olson, A. H., J. A. Orcutt, and G. A. Frazier (1984). The discrete wavenumber/finite element method for synthetic seismograms, *Geophys. J. R. astr. Soc.*, 77, 421-460.

DWFE Greens Functions Vertical Component

Dip-Slip Source

DEPTH= 1.00

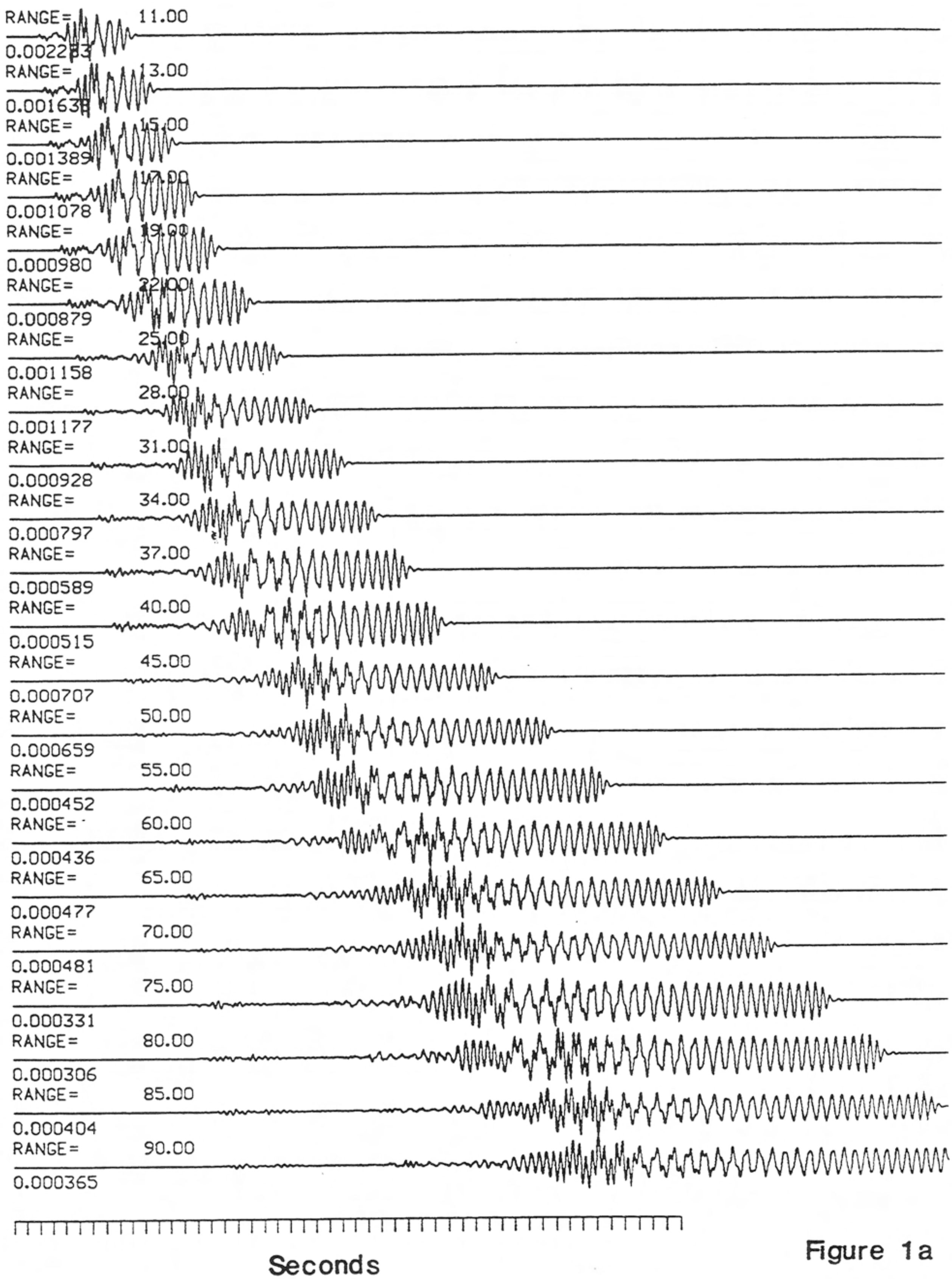

Figure 1a

DWFE Greens Functions Vertical Component

Dip-Slip Source

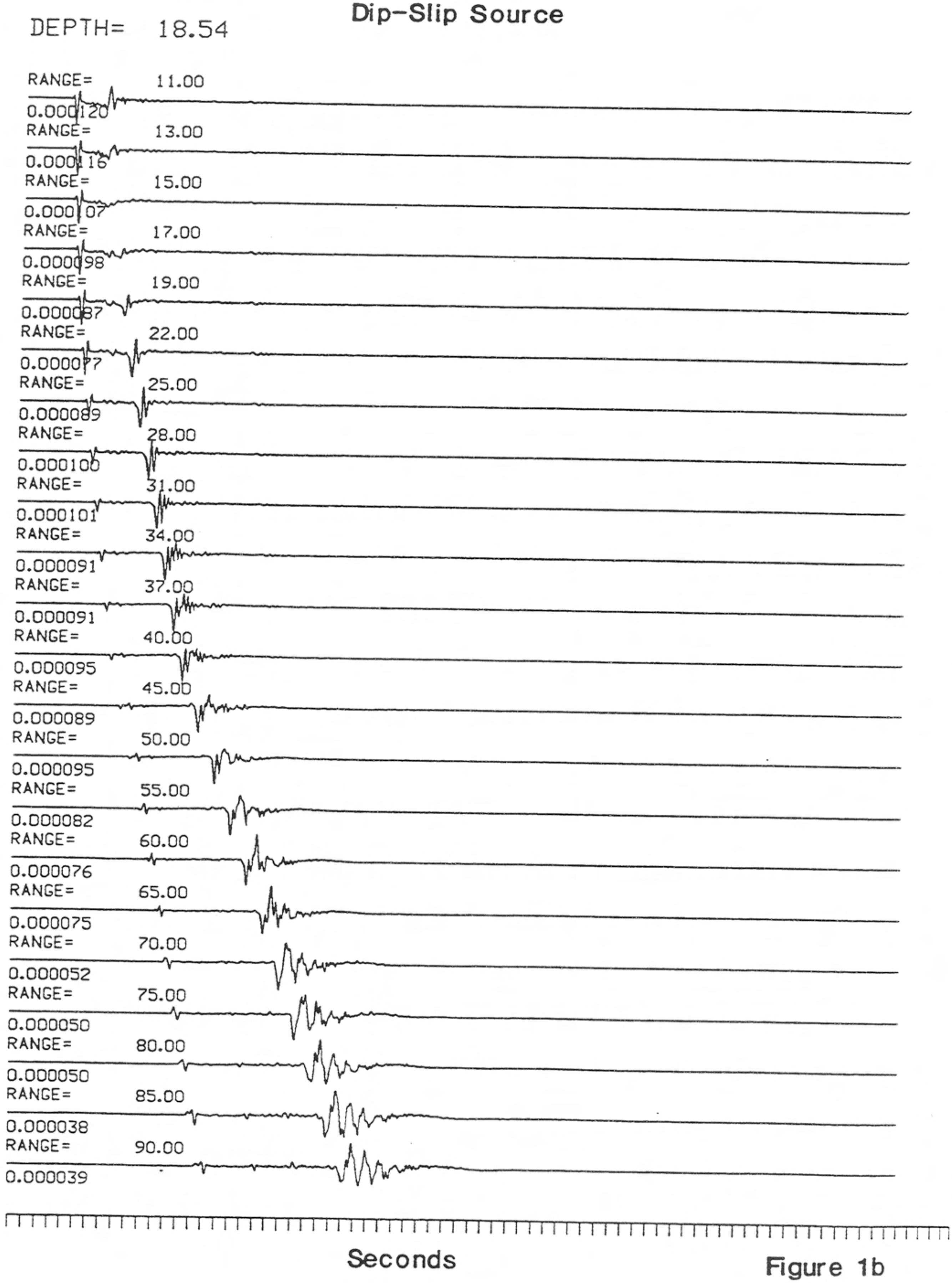

Figure 1b

Source-Time Function

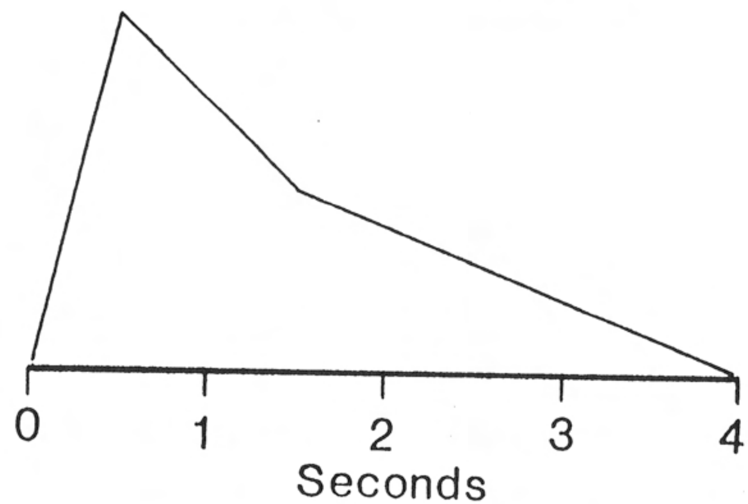

Rupture Front Contours - 3 Second Intervals

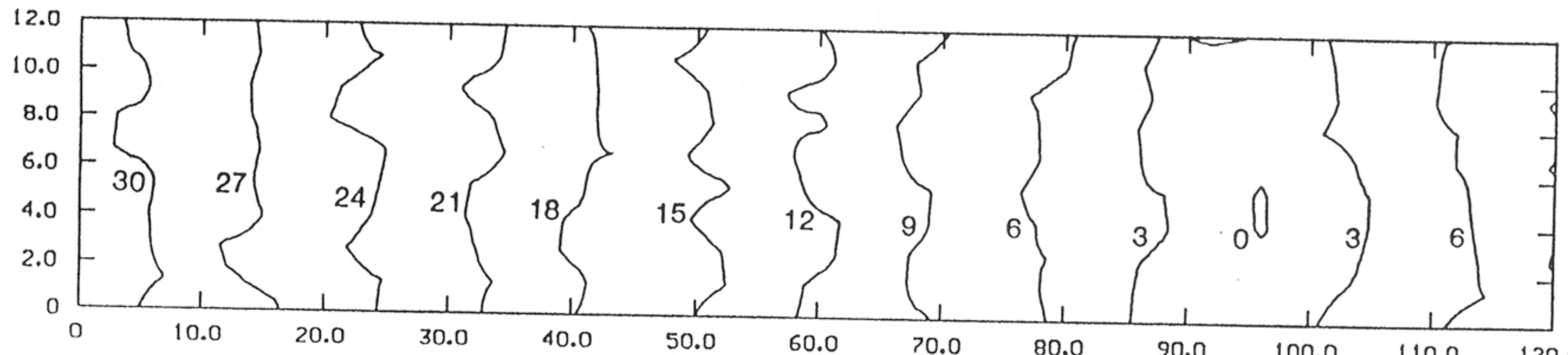

Figure 2

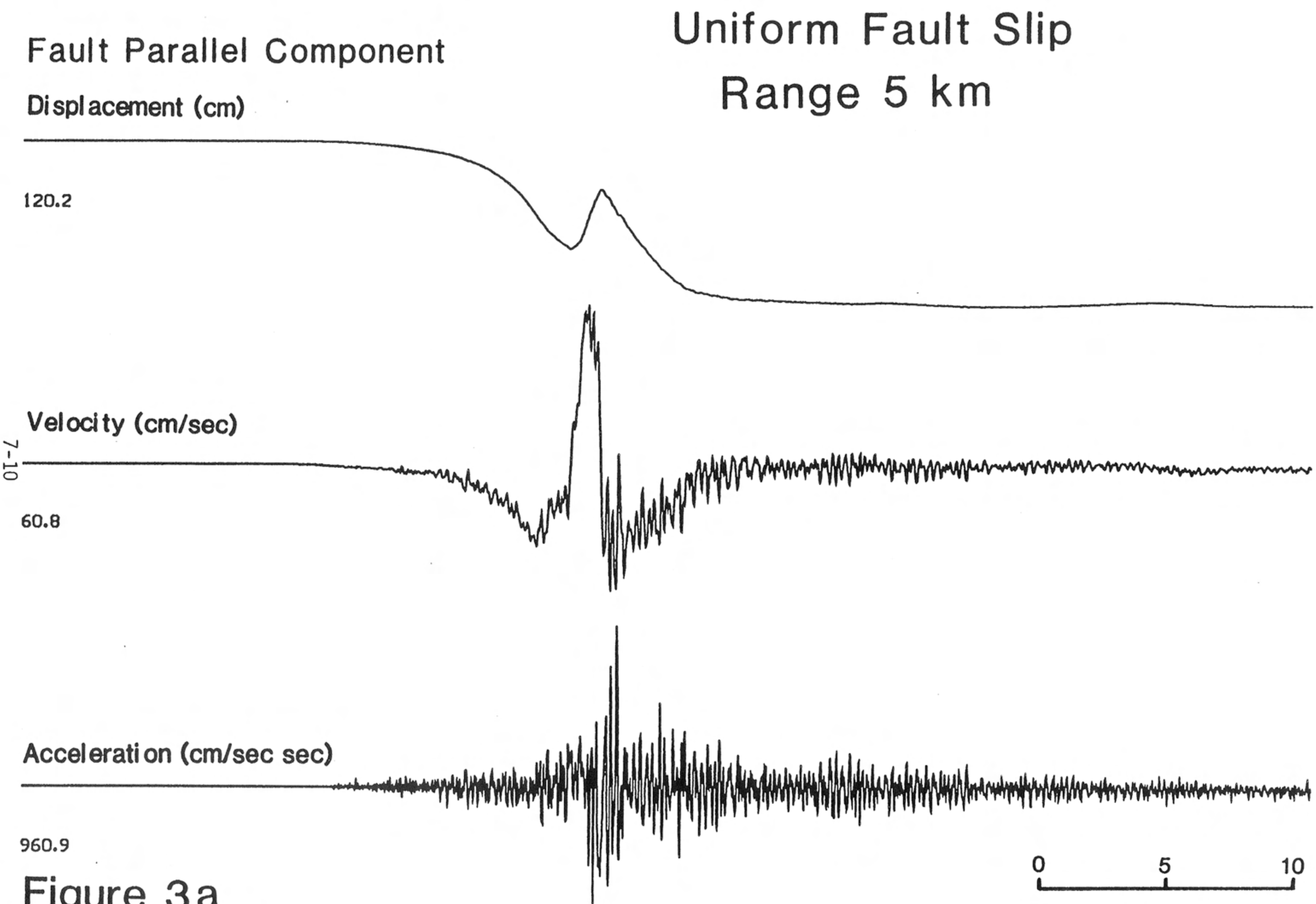

Uniform Fault Slip
Range 5 km
Fault Parallel Component
Displacement (cm)
120.2
Velocity (cm/sec)
60.8
Acceleration (cm/sec sec)
960.9
0
5
10
Seconds

Figure 3a

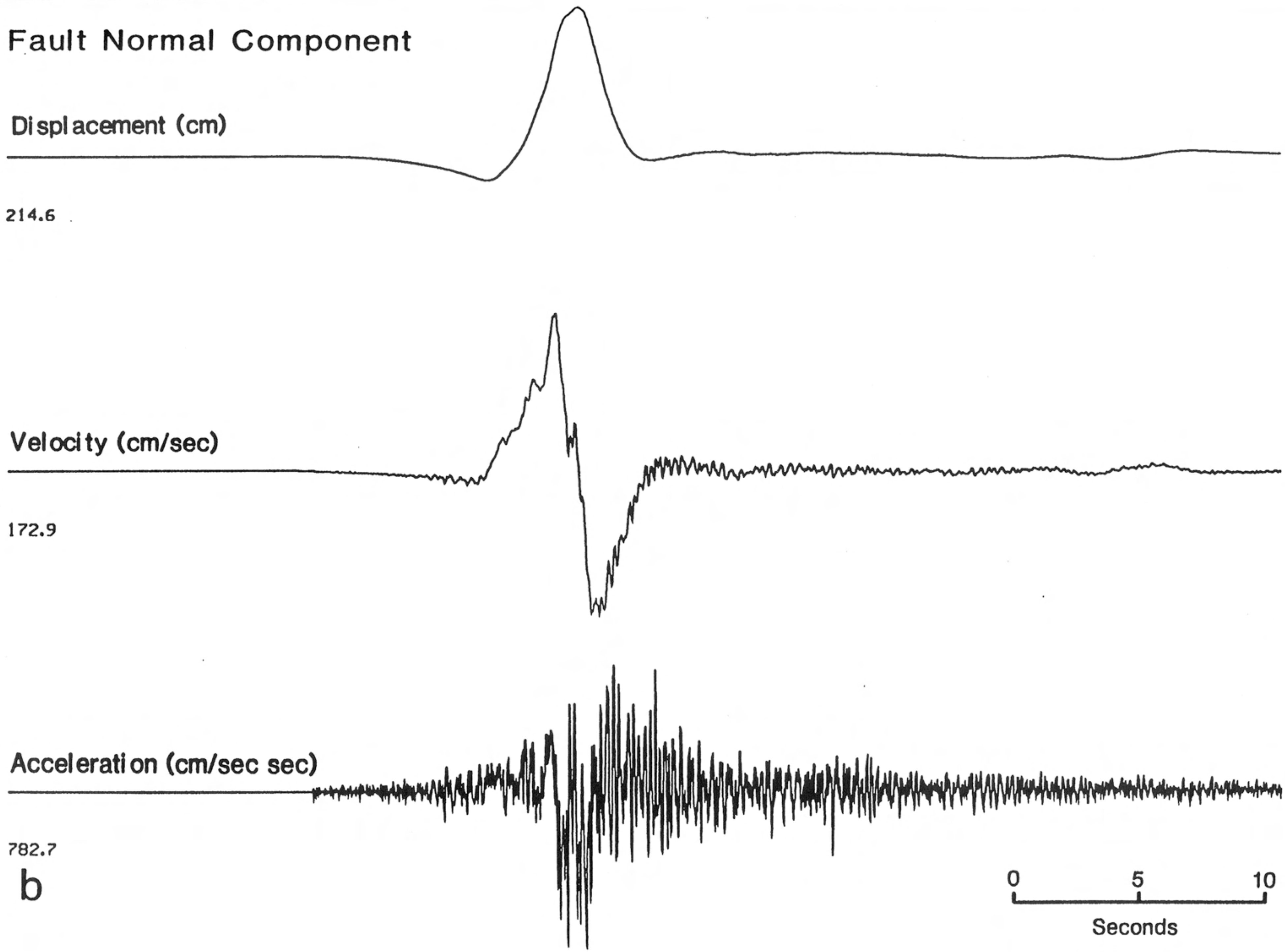
Fault Normal Component
Displacement (cm)
214.6
Velocity (cm/sec)
172.9
Acceleration (cm/sec sec)
782.7
b
0
5
10
Seconds

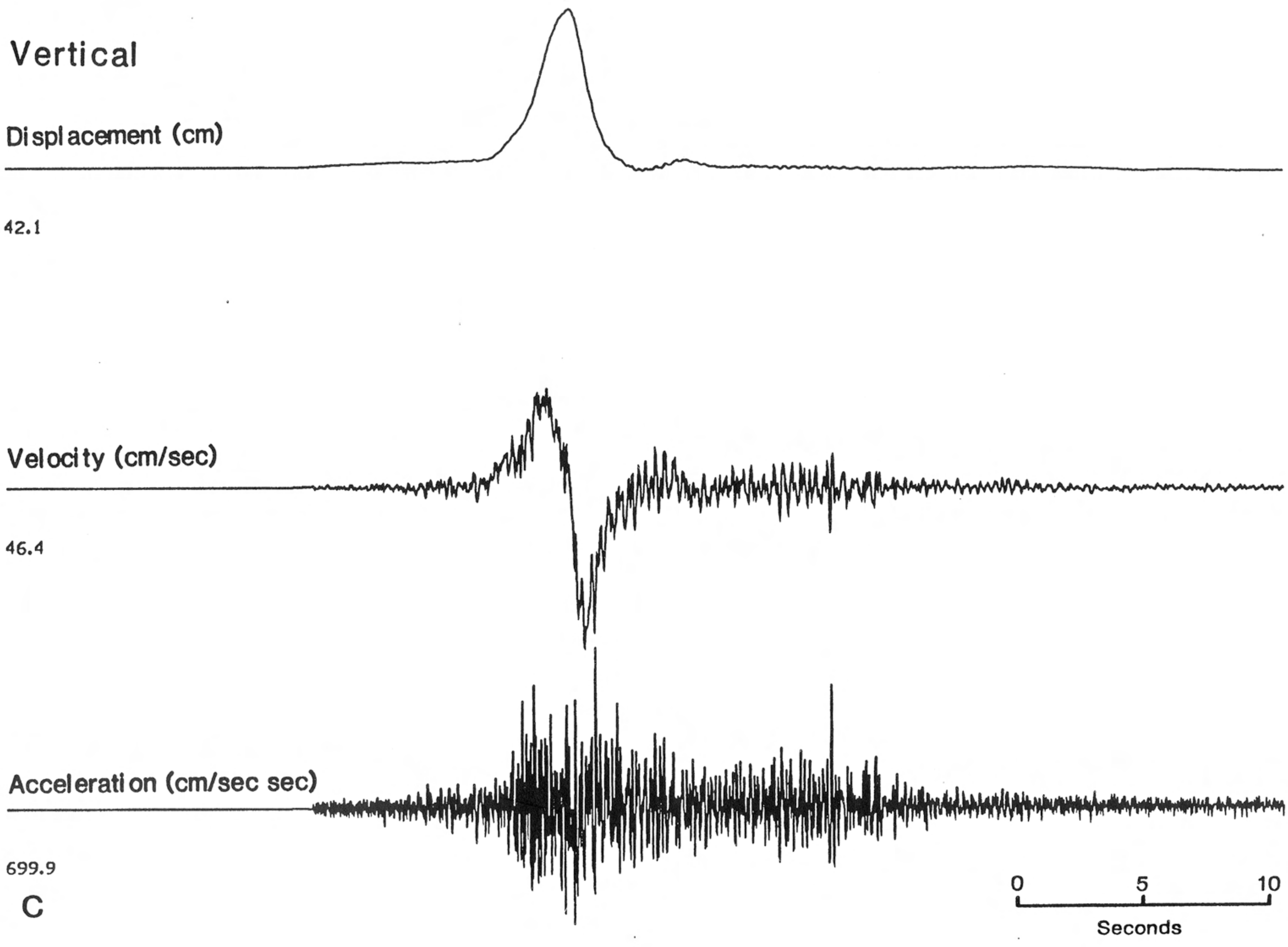

Vertical
Displacement (cm)
42.1
Velocity (cm/sec)
46.4
Acceleration (cm/sec sec)
699.9
C
0
5
10
Seconds

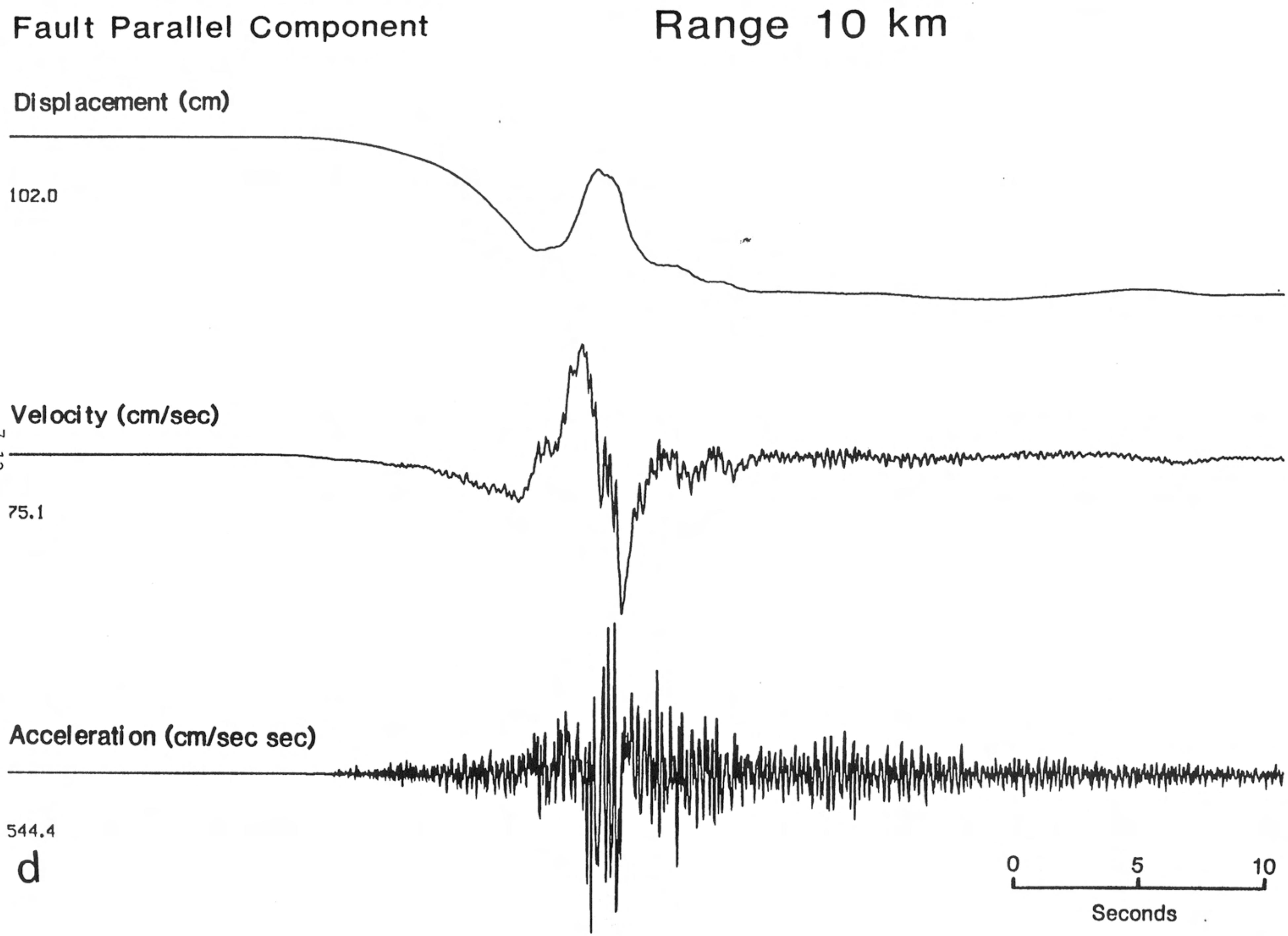
Fault Parallel Component
Range 10 km
Displacement (cm)
102.0
Velocity (cm/sec)
75.1
Acceleration (cm/sec sec)
544.4
d
0
5
10
Seconds

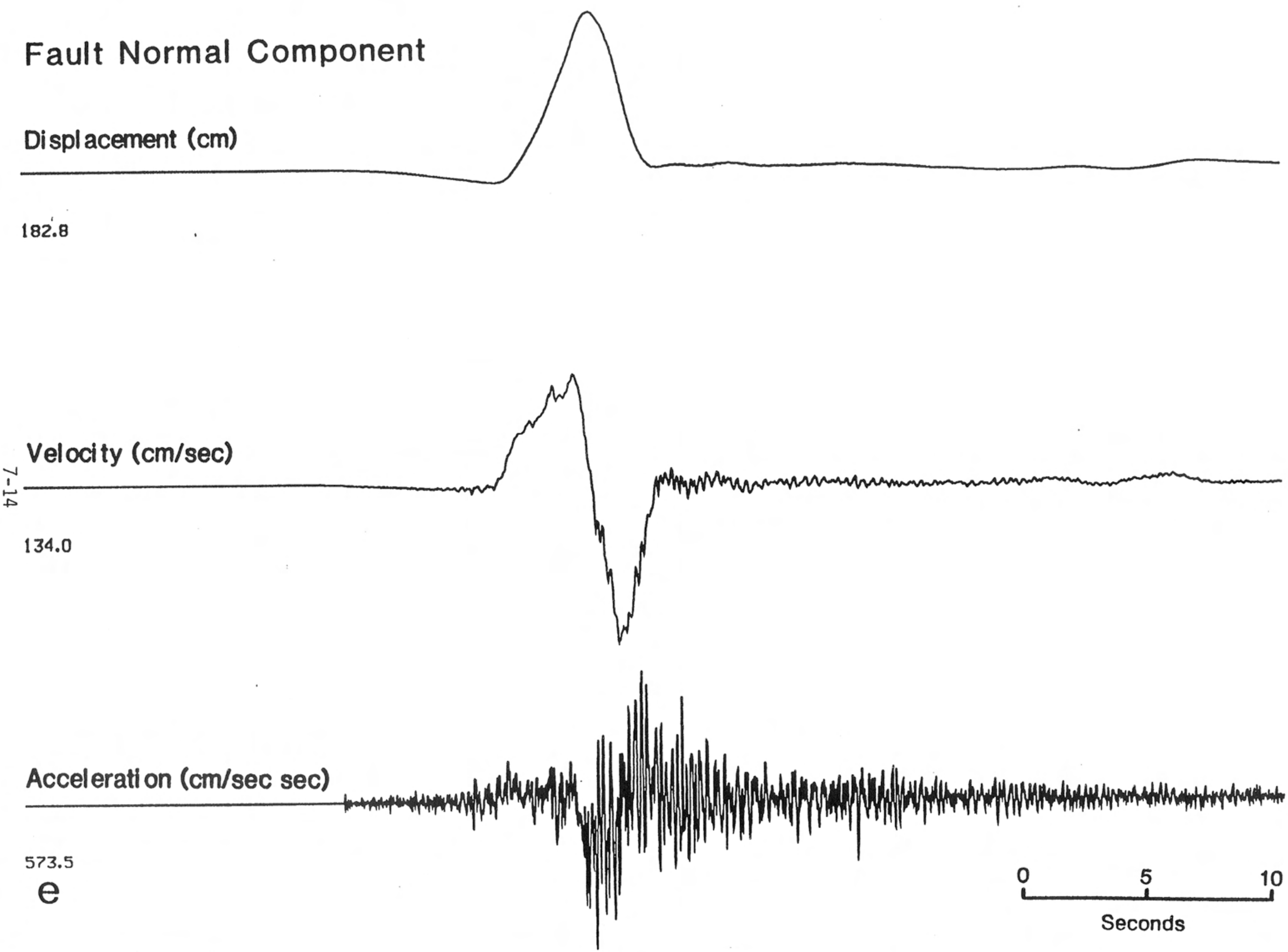
Fault Normal Component
Displacement (cm)
182.8
Velocity (cm/sec)
134.0
Acceleration (cm/sec sec)
573.5
e
0
5
10
Seconds

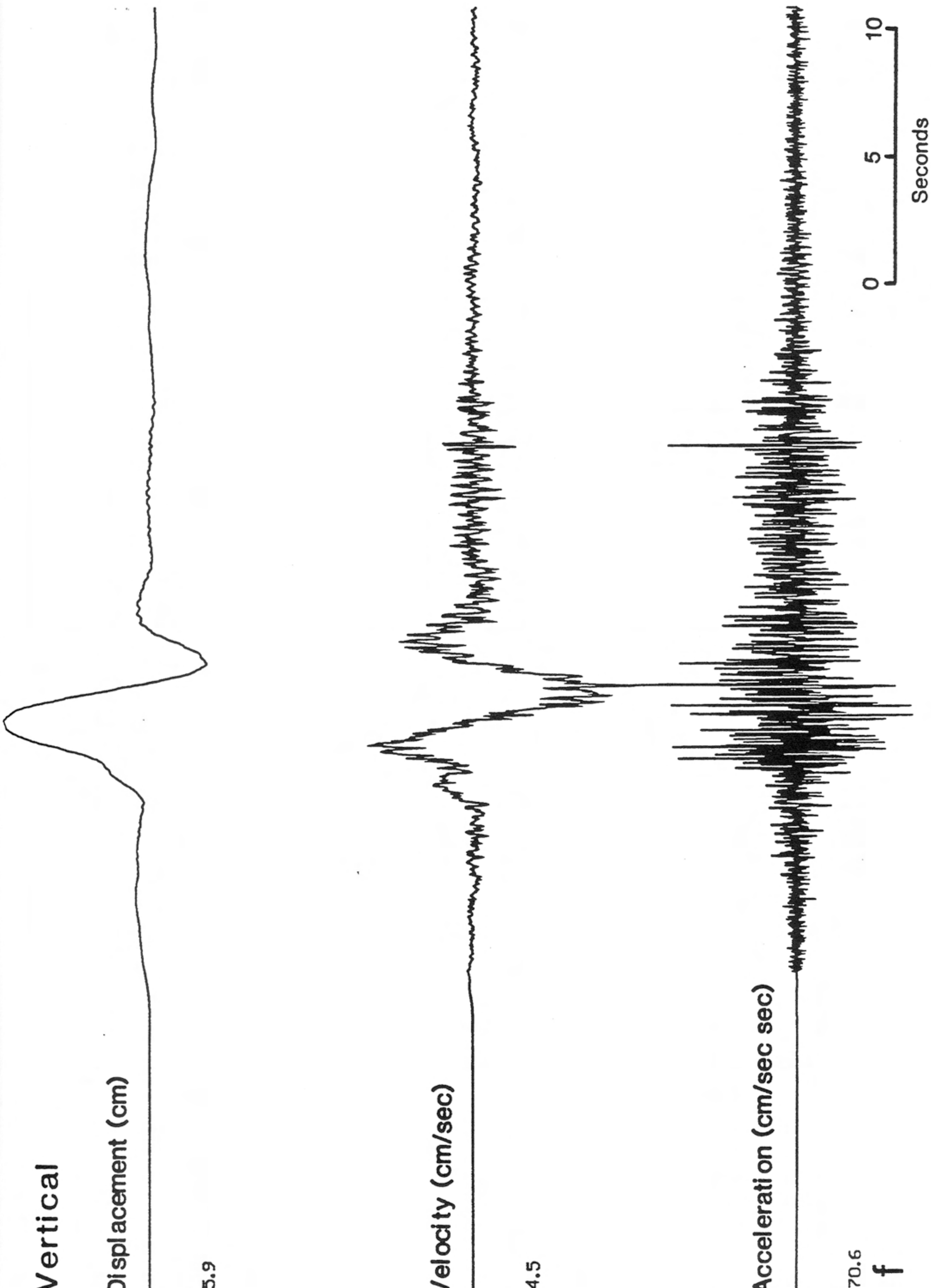
Vertical
Displacement (cm)
25.9
Velocity (cm/sec)
34.5
Acceleration (cm/sec sec)
470.6
f
0
5
10
Seconds

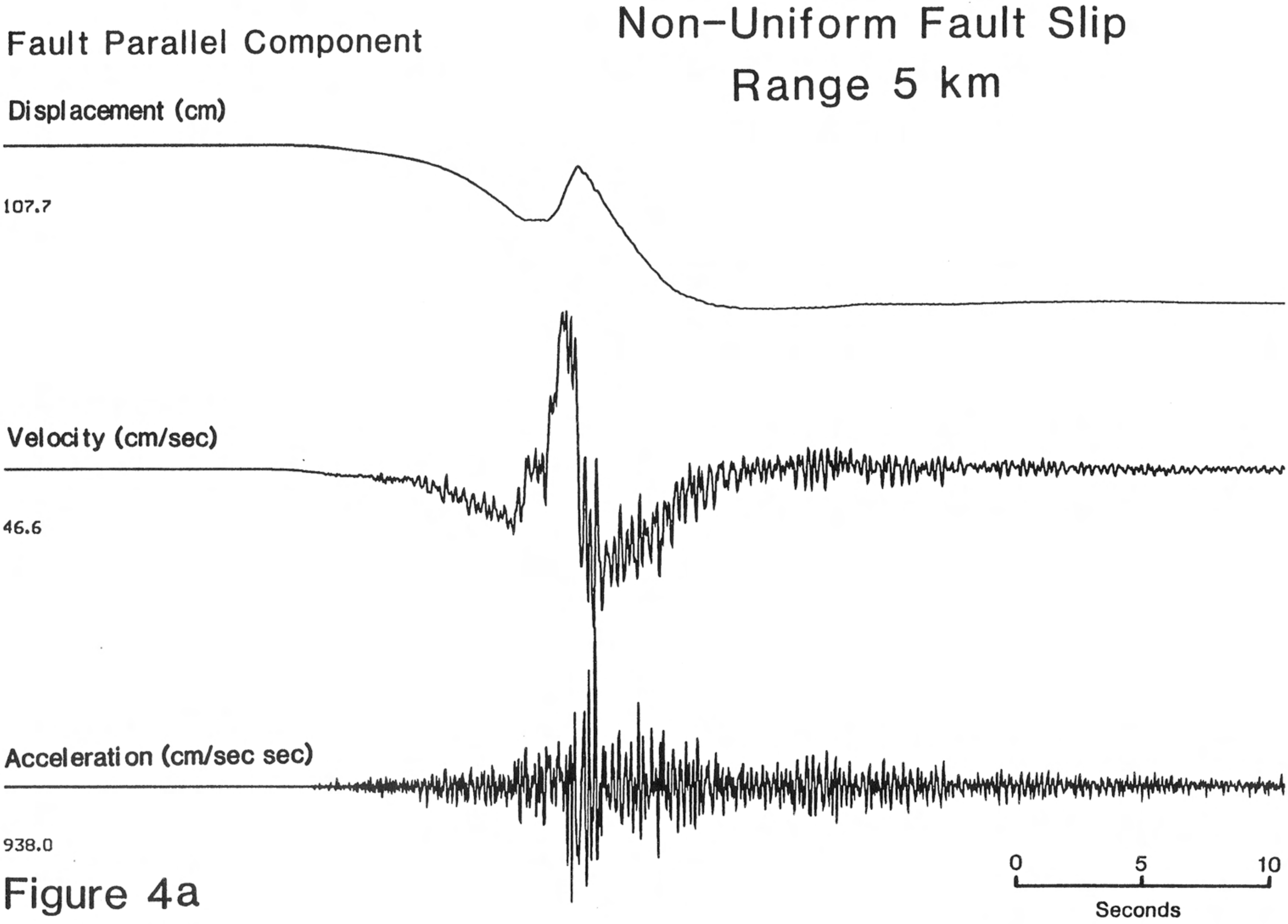
Fault Parallel Component
Non-Uniform Fault Slip
Range 5 km
Displacement (cm)
107.7
Velocity (cm/sec)
46.6
Acceleration (cm/sec sec)
938.0
0
5
10
Seconds

Figure 4a

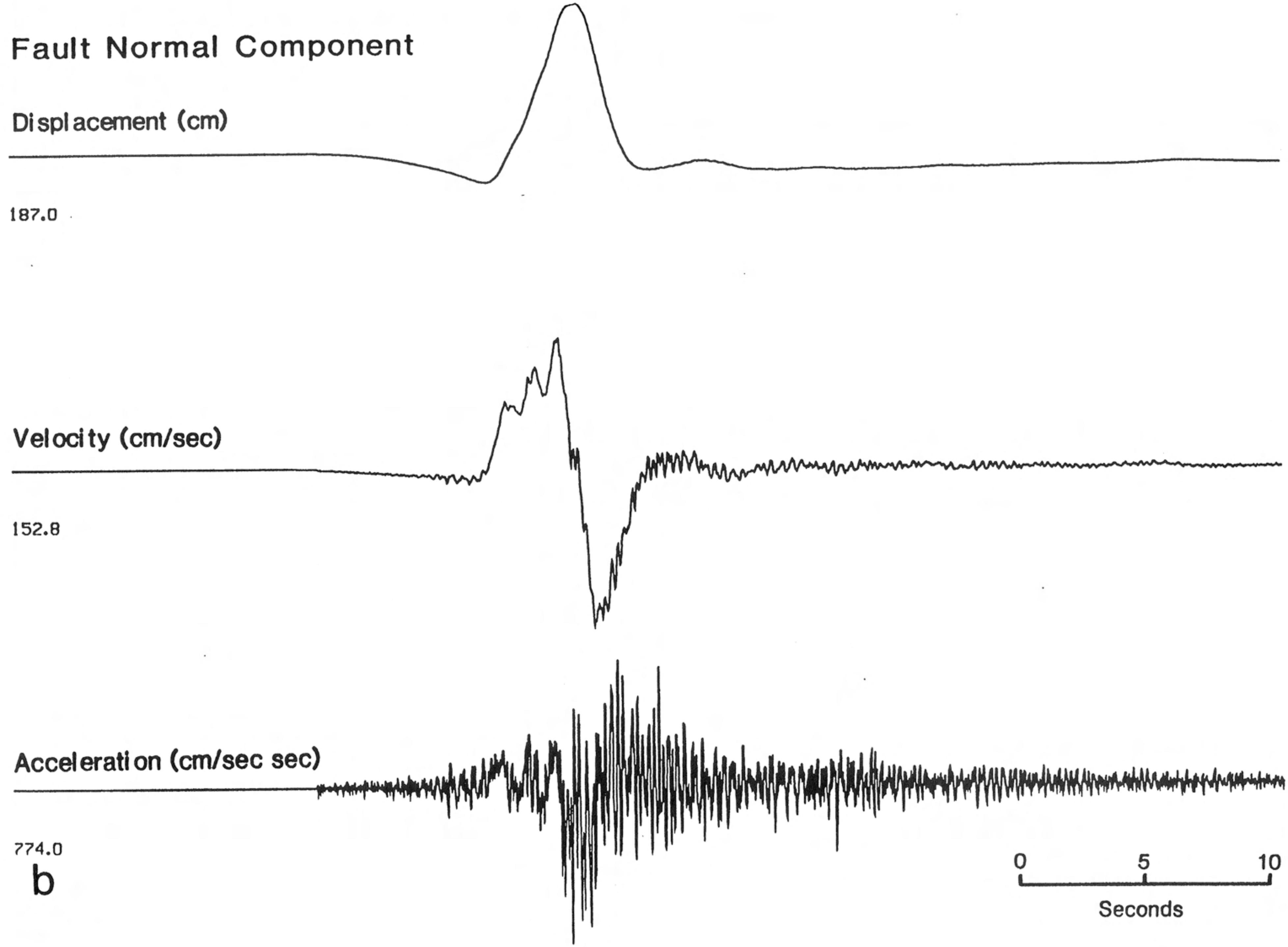
Fault Normal Component
Displacement (cm)
187.0
Velocity (cm/sec)
152.8
Acceleration (cm/sec sec)
774.0
b
0
5
10
Seconds

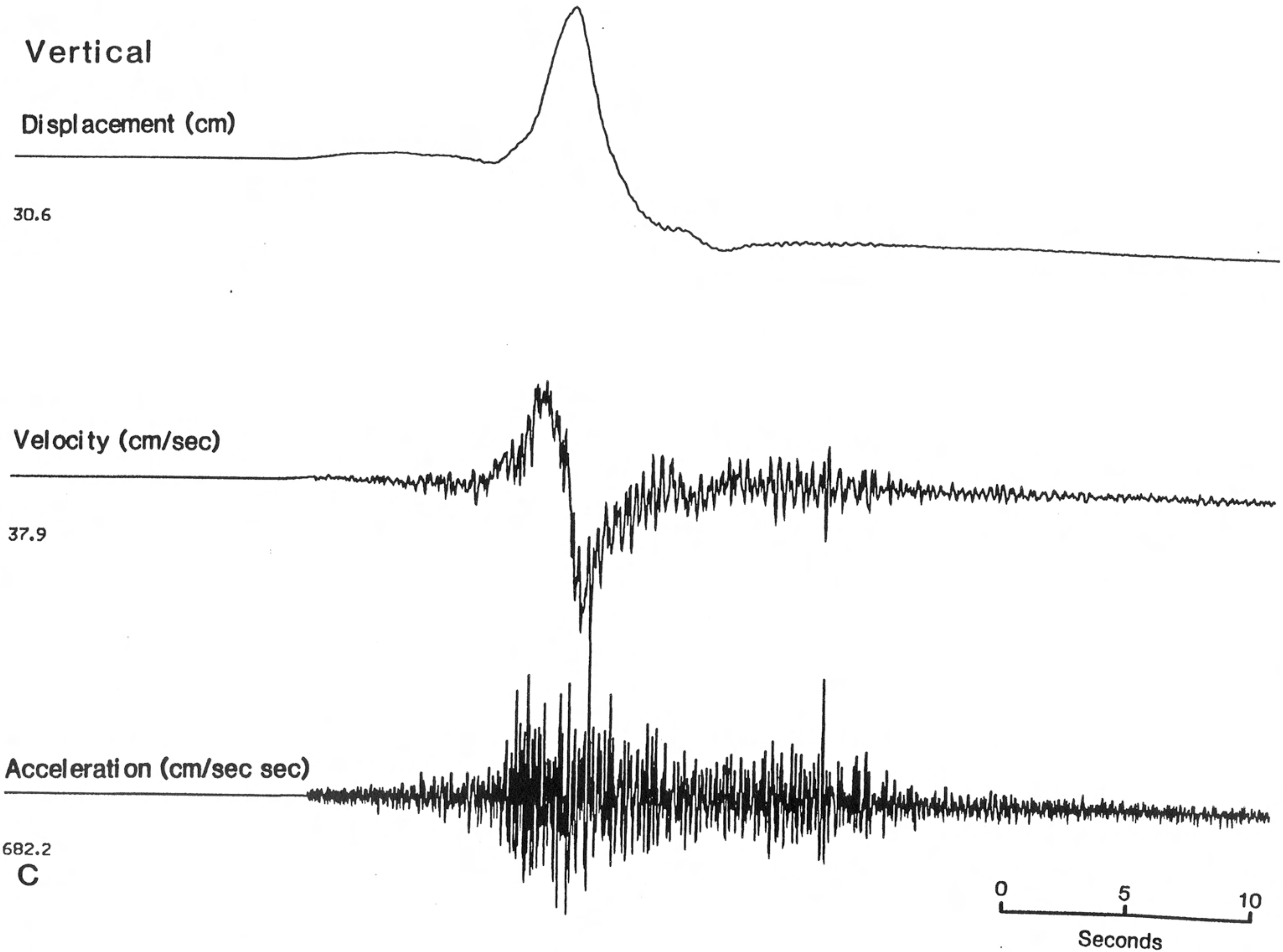
Vertical
Displacement (cm)
30.6
Velocity (cm/sec)
37.9
Acceleration (cm/sec sec)
682.2
C
0
5
10
Seconds

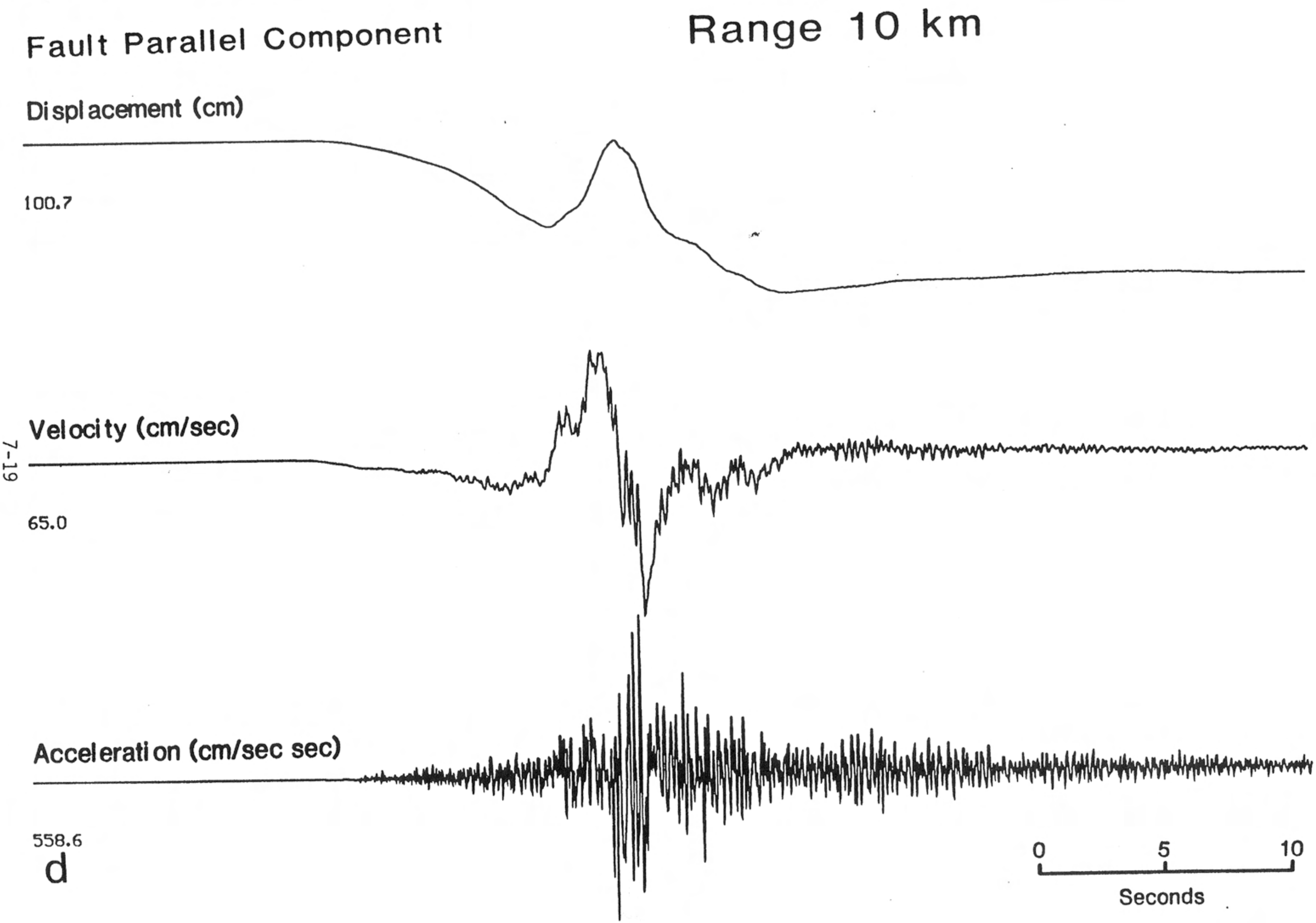
Fault Parallel Component
Range 10 km
Displacement (cm)
100.7
Velocity (cm/sec)
65.0
Acceleration (cm/sec sec)
558.6
d
0
5
10
Seconds

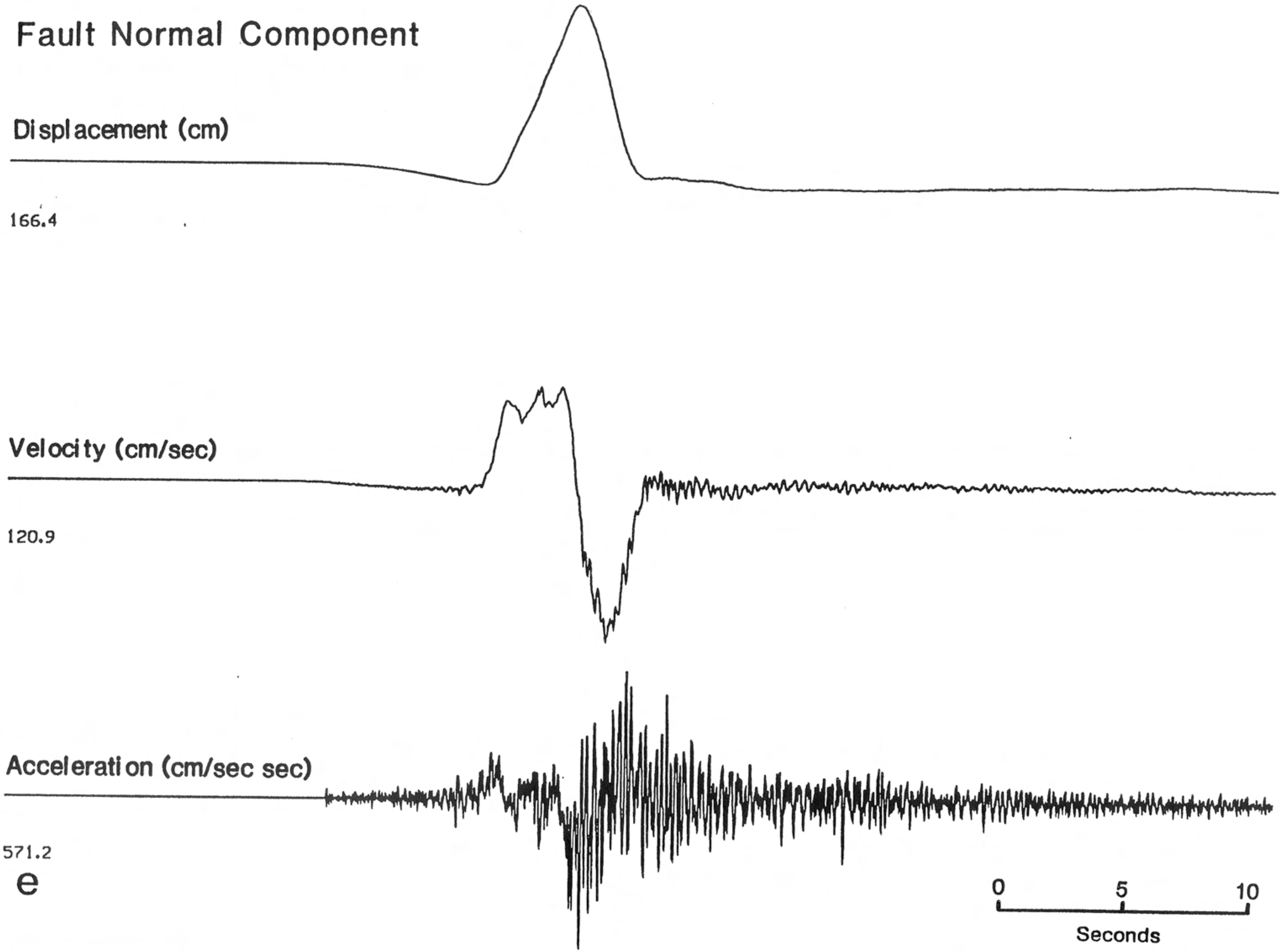
Fault Normal Component
Displacement (cm)
166.4
Velocity (cm/sec)
120.9
Acceleration (cm/sec sec)
571.2
e
0
5
10
Seconds

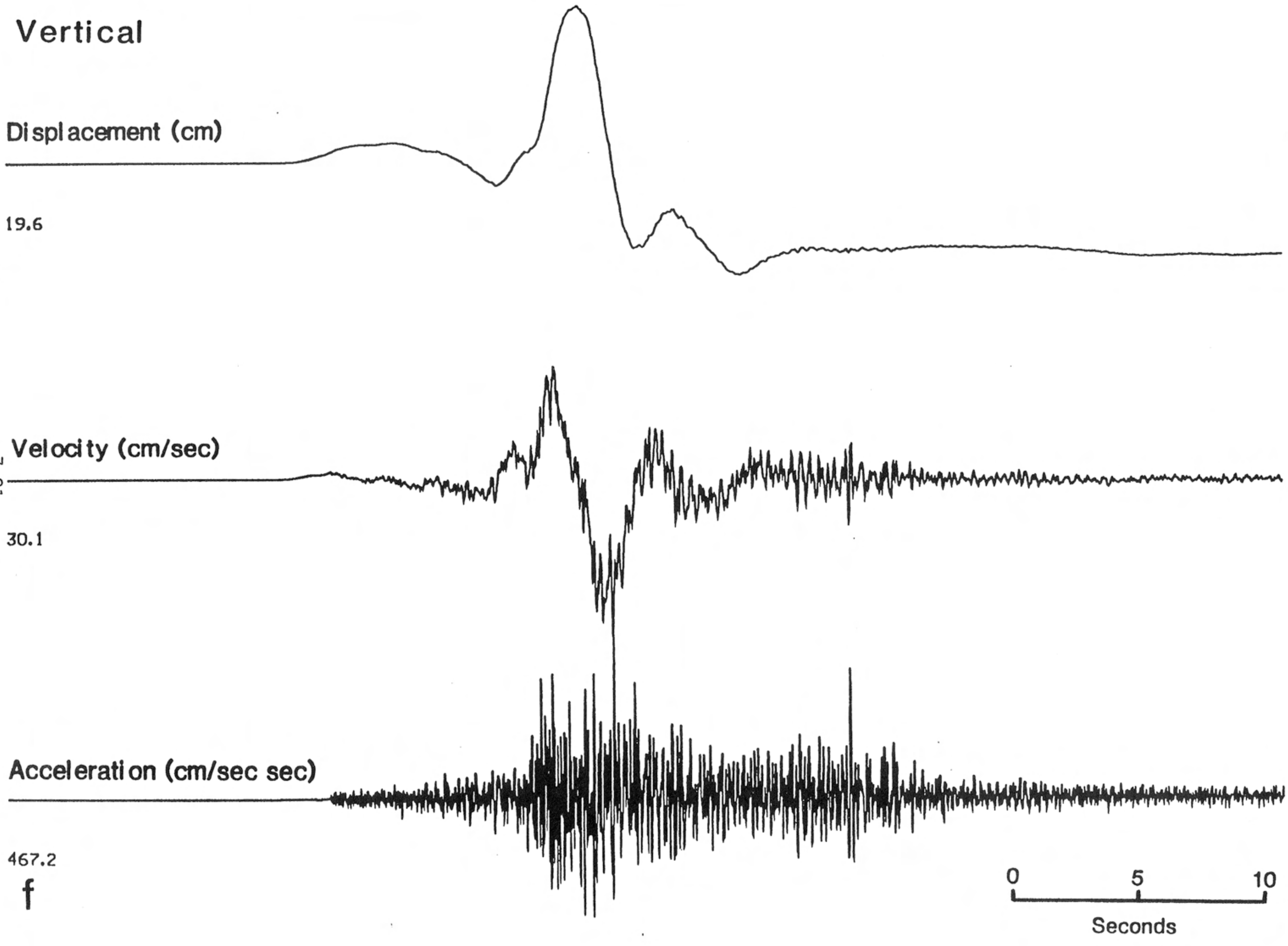
Vertical
Displacement (cm)
19.6
Velocity (cm/sec)
30.1
Acceleration (cm/sec sec)
467.2
f
0
5
10
Seconds